TRANSVERSE ECHOS IN RHIC*

W. Fischer and B. Parker, BNL, USA
O. Brüning, CERN, Switzerland

Abstract

Echo phenomena are well known in plasma physics and have been observed in accelerators in the longitudinal plane. Echo measurements are appealing since they allow the determination of small diffusion coefficients in a relatively short time. In this paper we explore the possibility of observing transverse echos in RHIC, created by a dipole kick followed by a quadrupole kick. We describe a technical solution for a pulsed quadrupole, present analytical estimates and show simulations of echo signals.

1 INTRODUCTION

Well known in plasma physics, echo phenomena have only been recently introduced to accelerator physics. First measurements of longitudinal echo signals have been reported [1–8].

In the simplest case, a transverse echo is generated by a dipole kick followed by a quadrupole kick. The echo signal appears as a dipole moment long after the initial dipole oscillations have disappeared. We consider only this case. Fig. 1–2 illustrate the creation of such an echo signal in normalized phase space. A particle distribution is displaced by several σ of the transverse beam distribution through a dipole kick. If the particle tune is amplitude dependent the distribution filaments but information on the phase relations between the particles is still retained if the filamentation time is not too long. A quadrupole kick after time τ changes the distribution although it does not affect the dipole moment. After a time $\tau_{echo} = 2\tau$ a transient dipole moment appears, the echo signal. The left hand side of Fig. 3 shows the dipole moment of the same distribution with a dipole kick only and the right hand side of Fig. 3 shows the dipole moment with an additional quadrupole kick, thus creating an echo signal. Such a signal can be observed with beam position monitors.

A particularly interesting aspect of echo measurements is the possibility of diffusion coefficient measurements in short time intervals since any form of diffusion reduces the echo signal.

One reason for the lack of transverse echo measurements is the difficulty of applying a short quadrupole kick to the beam. In the following section we will review the technical options of applying one-turn dipole and one-turn quadrupole kicks in RHIC. The next sections determine the expected maximum echo signal from theoretical computations and simulations. We consider the case of RHIC in proton operation at injection. In proton operation intrabeam scattering is less destructive to echo signals than in gold operation. At injection energy the quadrupole kick is most effective.

* Work performed under the auspices of the US Department of Energy.

2 RHIC INSTRUMENTATION FOR TRANSVERSE ECHOS

This section describes the possibilities of applying dipole and quadrupole kicks in RHIC as well as the detectors that can record an echo signal. While dipole kickers and detectors are installed and available the quadrupole kicker is still under construction.

2.1 Dipole Kickers

In RHIC there are three types of dipole kickers available: the injection kickers [9, 10], the tune kickers [11] and the abort kickers [12]. Their properties are summarized in Tab. 1. Only the injection kickers can provide a one-turn kick of several σ and restricts our investigations to the vertical plane. However, a dipole kick can also been achieved, by injecting the beam under an angle.

Table 1: RHIC dipole kickers at injection energy.

Kicker	Strength range		Kick length
	[μrad]	σ	
Injection (ver)	300–1500	4.7–23.5	60 ns
Tune (hor)	0–11	0–0.2	90 ns
Tune (ver)	0–11	0–0.1	90 ns
Abort (hor)	250–2500	4.2–390	> 12 μs

2.2 Quadrupole Kicker

The quadrupole kicker is the real challenge in producing transverse echos. We have available a special air core quadrupole magnet [13] that can be used for a quadrupole kicker. This magnet had been installed at the IP4 interaction region and is common to both rings.

The magnet is designed for a maximum current of 50 A which corresponds to a focal length of 500 m at injection energy. However, in pulsed operation the current could be raised above the 50 A design value.

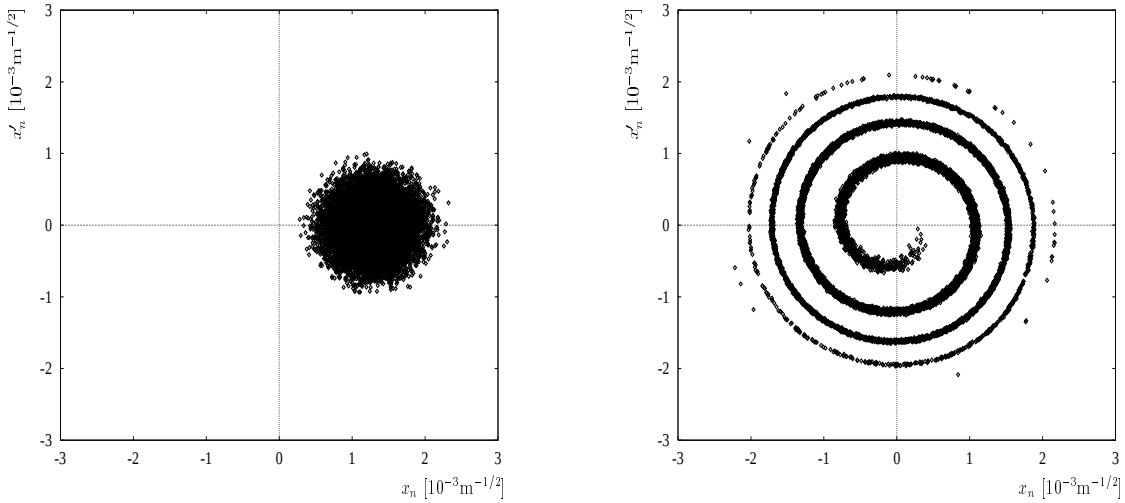

Figure 1: Left: Horizontal particle distribution in normalized phase space after the initial dipole offset. Right: The same distribution 500 turns later.

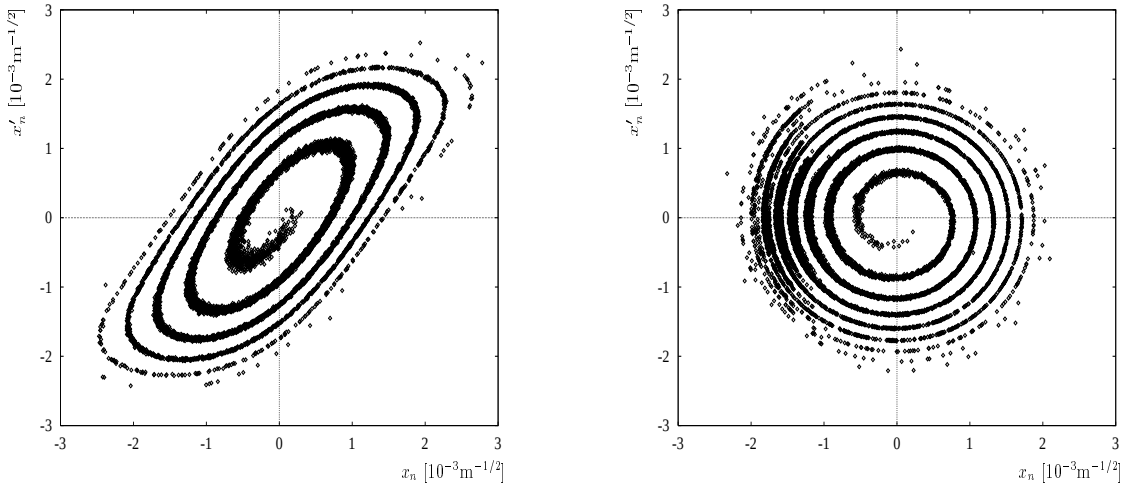

Figure 2: Left: Horizontal particle distribution in normalized phase space right after a 1 turn long quadrupole kick placed 500 turns after the dipole kick. Right: The same distribution 500 turns after the quadrupole kick.

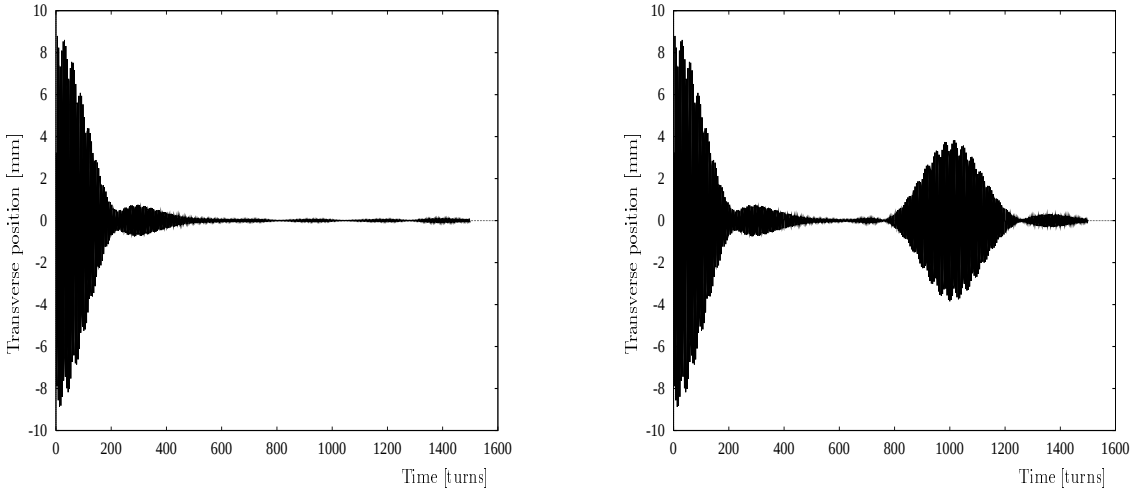

Figure 3: Left: The dipole moment of the distribution versus time after a dipole kick. Right: The same signal with an additional quadrupole kick at 500 turns after the dipole kick.

Fig. 4 shows resistance and Fig. 5 the inductance measurements for the quadrupole as a function of frequency. In one case it is assumed that resistance and inductance are in series while in the other case it is assumed that they are in parallel. In the parallel case the inductance is relatively constant at 125 μH up to a frequency of 1 kHz and drops to about 105 μH at a frequencies beyond 1 kHz. A one-turn pulse would correspond to a frequency of 20kHz.

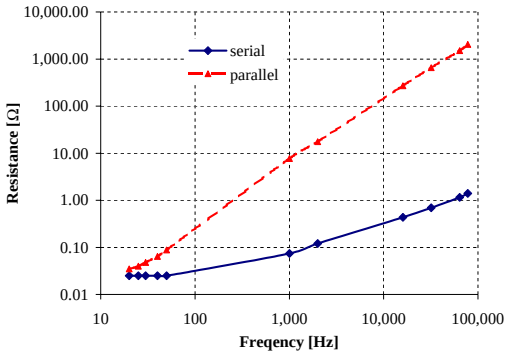

Figure 4: Resistance measurements of the quadrupole. Results labeled "serial" assume that resistance and inductance are in series, results labeled "parallel" assume that resistance and inductance are in parallel.

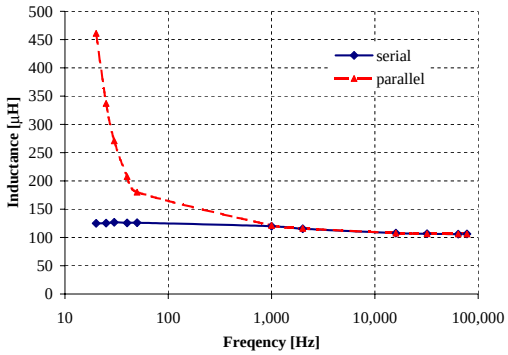

Figure 5: Inductance measurement of the quadrupole. Results labeled "serial" assume that resistance and inductance are in series, results labeled "parallel" assume that resistance and inductance are in parallel.

A relatively simple design for the pulsed operation of the quadrupole is the one shown in Fig. 6. By closing the switch $S1$ a power supply charges the capacitor C. When charged the switch $S1$ opens again. By closing the switch $S2$ at the time t_0 the capacitor C will start to discharge over the quadrupole with the inductance $L = 105$ μH. We neglect for the moment magnet and cable resistance as well as switching time.

The current in the coil L reaches a maximum after the time t_1 when the switch $S2$ can be opened again. The energy stored in the coil is then discharged in the resistor R. By choosing R appropriately the current in the coil can be zero after the time t_2 with little further oscillation. During the time $t_2 - t_0$ there is a field in the quadrupole that would create a quadrupole kick. The time $t_2 - t_0$ can therefore be

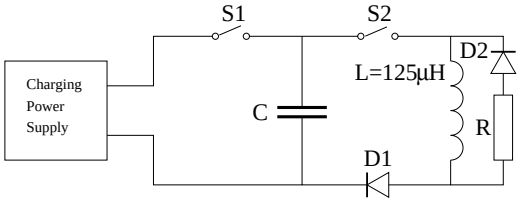

Figure 6: Electric circuit for a pulsed quadrupole.

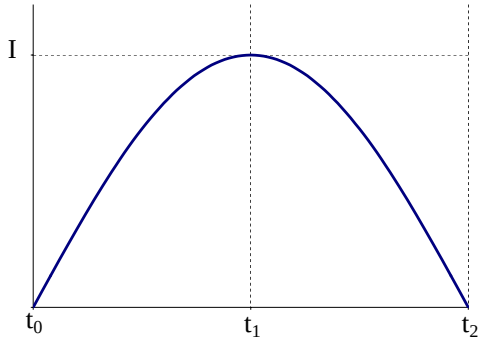

Figure 7: Current in the coil L after the switch $S2$ is closed.

2 turns long, one turn to raise the current and one turn to bring it to zero again.

For the angular frequency ω_0 of the electric circuit, the capacitance C and the voltage V over the coil L the relations

$$\omega_0 = \frac{2\pi}{2(t_2 - t_0)}, \quad C = \frac{1}{\omega_0^2 L} \quad \text{and} \quad V = \omega_0 L I. \tag{1}$$

hold. Fig. 8 shows the capacitance C and the voltage V as a function of the quadrupole kick length assuming that the peak current I_{max} in the coil is 50 A. According to Eq. (1) the voltage over the quadrupole will increase proportionally with the current, which in turn is proportional to the quadrupole kick strength.

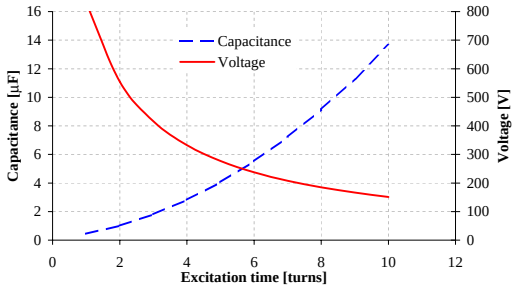

Figure 8: Capacitance and voltage as a function of the quadrupole excitation time for a peak current of 50 A in the quadrupole.

2.3 Detectors

For the observation of transverse echos only beam position monitors (BPMs) are needed. The RHIC arc BPMs are located at positions where the β-function reaches a local maximum of 48m. The arc BPMs have a resolution of at least 0.1 mm if there are no less than 10^9 charges per bunch [14]. For protons this is about 1% of the design intensity [15]. The detection of echo signals of several millimeters should therefore pose no problem.

During the RHIC commissioning a turn-by-turn ionization profile monitor (IPM) has been tested successfully [16]. While the BPMs can only detect the center of charge, the IPM would give the projection of the phase space distribution onto the x- or y-axis.

3 ANALYTICAL ESTIMATES OF ECHO SIGNALS

In this section we follow closely Ref. [17]. We use normalized phase space coordinates (x_N, x'_N) according to

$$x_N = \frac{1}{\sqrt{\beta}}\, x \;\text{ and }\; x'_N = \frac{1}{\sqrt{\beta}}(\alpha x + \beta x') \qquad (2)$$

where (x, x') are the unnormalized transverse phase space coordinates and α and β are the lattice functions. The initial particle distribution is assumed to be Gaussian with an rms emittance ϵ:

$$\psi(x_N, x'_N) = \frac{1}{2\pi\epsilon}\exp\left\{\frac{x_N^2 + {x'_N}^2}{2\epsilon}\right\} \qquad (3)$$

We furthermore define Q as the ratio of the β-function at the quadrupole location to the focal length of the quadrupole, a the dipole kick strength in normalized coordinates and τ the time between dipole and quadrupole kick. μ gives the amplitude dependent tune shift at one σ of the unkicked particle distribution,

$$\nu = \nu_0 - \mu\frac{x_N^2 + {x'_N}^2}{\epsilon}. \qquad (4)$$

Second order perturbation theory gives for the echo amplitude $\eta = \sqrt{x_N^2 + {x'_N}^2}$ after a one-turn dipole and a one-turn quadrupole kick

$$\eta = aF\left(\frac{\tau}{\tau_0}\frac{t-\tau}{\tau_d}\right) \qquad (5)$$

where $\tau_0 = Q\tau$, $\tau_d = T_0/4\pi\mu$ and the function F

$$F(x,y) = \frac{x}{[(1+x^2-y^2)^2 + 4y^2]^{2/3}}. \qquad (6)$$

The effect of diffusion on the echo amplitude can be computed for the case when the time τ is small compared to the decoherence time τ_d and the parameter Q is small [18]. In this case one has

$$\eta^{max} = \frac{aQ}{\tau_d}\frac{\tau}{1 + 8D_0\mu^2\omega_0^2\tau^3/3\epsilon}, \qquad (7)$$

where $\omega_0 = 2\pi/T_0$ is the angular revolution frequency and D_0 the diffusion coefficient. For the parameters in Tab. 2 Eq. (7) gives a maximum echo amplitude of 0.44 of the dipole kick and 5000 turns between the dipole and the quadrupole kick. Such an echo amplitude would be observable.

4 SIMULATIONS

In the simulations we assume that the quadrupole kick can be extended over a few turns. This mode of operation is not covered in Sec. 3. The simulations are used to determine the maximum acceptable kick length of a pulsed quadrupole kick, the optimum time τ between dipole and quadrupole kick and the minimum required kick amplitude. In all cases we assume that the quadrupole signal increases over half the kick length (ramp-up) reaches its maximum signal at half the kick length and decreases again during the second half of the kick length (ramp-down).

The left hand side of Fig. 9 shows such an excitation versus time. The right hand side of Fig. 9 shows the maximum echo response (dipole signal) versus the excitation time ΔT for a quadrupole kick 5,000 turns after the dipole offset with an quadrupole kick amplitude corresponding to 25A. The signal decreases rapidly for a pulsed excitation which is longer than 10 turns. Note that dipole kick was 9 mm and the computed echo amplitude for one turn from Eq. (7) is 2 mm in agreement with the simulation.

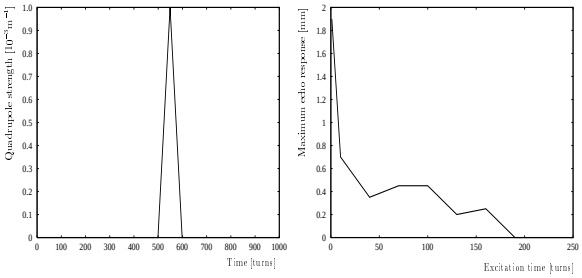

Figure 9: Left: The quadrupole excitation versus time for a amplitude of $k = 1.0 \cdot 10^{-3}\mathrm{m}^{-1}$ and an excitation time of 100 turns. Right: The maximum echo response versus the excitation time ΔT.

Because the particle distribution rotates in the transverse phase space with the betatron frequency a long quadrupole excitation does not lead to a simple elongation and tilt of the phase space distribution but rather to a perturbation which looks approximately uniform over the azimuthal angle of the transverse phase space. Since the echo signal relies on local density deformation along the azimuthal angle of the transverse phase space this uniformity of the distribution reduces the final echo amplitude. For a perfectly uniform azimuthal perturbation of the transverse distribution the echo signal vanishes entirely.

The left hand side of Fig. 10 shows the maximum echo response versus the time separation between the initial dipole offset and a 10 turn long quadrupole kick. The echo

Table 2: RHIC machine parameters, proton beam at injection.

Parameter	Symbol	Unit	Value
Revolution frequency	f_{rev}	kHz	78.196
Particle momentum	p	GeV/c	25
Maximum transverse rms beam size	$\sigma_{x,y}$	mm	2.42
Maximum transverse β-function in arcs	$\beta_{x,y}$	m	48.6
Transverse tune	$\nu_{x,y}$	1	28.19/29.18
Detuning	μ	1	0.0035
Quadrupole kick strength (at 50A current)	Q	1	0.02

signal has a maximum amplitude for a time separation of 60,000 turns between the dipole kick and the quadrupole kick. Assuming that the maximum echo response varies linearly with the quadrupole excitation amplitude and requiring a maximum echo response of at least 1/10 of the initial 9 mm dipole signal one needs a quadrupole kick of

$$k \geq 1.8 \cdot 10^{-4}\mathrm{m}^{-1} \text{ and } \Delta T \leq 10 \text{ turns}. \qquad (8)$$

The right hand side of Fig. 10 shows the dipole signal of the distribution versus the number of turns for a 10 turn long quadrupole kick with $k = 1.0 \cdot 10^{-3}\mathrm{m}^{-1}$ at turn 50,000 after the initial dipole offset.

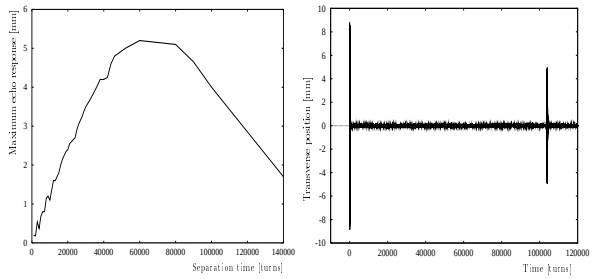

Figure 10: Left: The maximum echo response versus the separation time T between the initial dipole kick and a 10 turn long quadrupole kick with $k = 1.0 \cdot 10^{-3}\mathrm{m}^{-1}$. Right: The dipole signal of the distribution versus time for a 10 turn long pulsed quadrupole kick with $k = 1.0 \cdot 10^{-3}\mathrm{m}^{-1}$ at turn 50,000 after the initial dipole offset.

5 SUMMARY

It should be possible to built a quadrupole kicker for RHIC that gives a one-turn normalized quadrupole kick of $Q = 0.02$. Analytical estimates and simulations predict that with such a quadrupole kick a transverse echo should be overvable in at injection. Transverse echo measurement may allow the fast determination of diffusion coefficients.

6 REFERENCES

[1] T.M. O'Neil and R.W. Gould, Phys. Fluids **11**, 1 (1968).

[2] G. Stupakov, "Echo effect in hadron colliders", SSCL-579 (1992).

[3] G. Stupakov and S. Kauffmann, "Echo effect in accelerators", SSCL-587 (1992).

[4] N. Mahale et al., "Displaced bunch synchrotron oscillation echoes in accelerators", SSCL-N-817 (1993).

[5] L.K. Spentzouris, J.-F. Ostiguy and P.L. Colestock, "Direct measurement of diffusion rates in high energy synchrotrons using longitudinal beam echoes", PRL Vol. 76, No 4, pp. 620 (1996).

[6] O. Brüning, "On the possibility of measuring longitudinal echos in the SPS", CERN SL/95-83 (AP) (1995).

[7] O. Brüning et al., "Beam echos in the CERN SPS", proceedings of the 1997 Particle Accelerator Conference, Vancouver, (1997).

[8] J. Kewisch and M. Brennan, "Bunched beam echos in the AGS", proceedings of the 1998 European Particle Accelerator Conference, Stockholm (1998).

[9] W. Fischer et al., "Beam Injection into RHIC", proceedings of the 1997 Particle Accelerator Conference, Vancouver (1997).

[10] H. Hahn, J.E. Tuozzolo, "The RHIC injection kicker", proceedings of the 1997 Particle Accelerator Conference, Vancouver (1997).

[11] P. Cameron et al.,"ARTUS: A Rhic TUne monitor System", BNL RHIC/AP/156 (1998).

[12] H. Hahn et al., "The RHIC Beam Abort Kicker System", proceedings of the 1999 Particle Accelerator Conference, New York, (1999).

[13] W. Fischer, A. Jain and D. Trbojevic, "The AC quadrupole in RHIC", RHIC/AP/164 (1999).

[14] P. Cameron and T. Shea, private communication (1999).

[15] "RHIC Design Manual", revision of April 1998.

[16] P. Cameron et al., "The RHIC Ionization Beam Profile Monitor", proceedings of the 1999 Particle Accelerator Conference, New York, (1999).

[17] G.V. Stupakov, "Echo", in A.W. Chao and M. Tigner (editors), "Handbook of Accelerator Physics and Engineering", World Scientific (1999).

[18] G.V. Stupakov and A.W. Chao, "Effect of Diffusion on Bunched Beam Echo", proceedings of the 1997 Particle Accelerator Conference, Vancouver, (1997).